Journal of Colloid and Interface Science 477 (2016) 16–24

Contents lists available at ScienceDirect

Journal of Colloid and Interface Science

journal homepage: www.elsevier.com/locate/jcis

The surface state of hematite and its wetting characteristics

Kaustubh Shrimali, Jiaqi Jin, Behzad Vaziri Hassas, Xuming Wang, Jan D. Miller *

Department of Metallurgical Engineering, College of Mines and Earth Sciences, University of Utah, 135 South 1460 East, Room 412, Salt Lake City, UT 84112-0114, USA

GRAPHICAL ABSTRACT

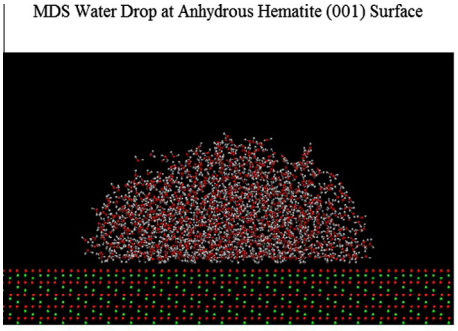

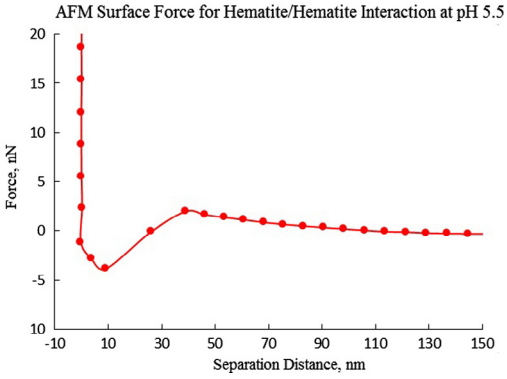

ARTICLE INFO

Article history:
Received 4 April 2016
Revised 16 May 2016
Accepted 17 May 2016
Available online 18 May 2016

Keywords:
Hematite
Goethite
Atomic force microscopy
Molecular dynamics simulation
Hydroxylation
Zeta potential

ABSTRACT

Apart from being a resource for iron/steel production, the iron oxide minerals, goethite and hematite, are used in the paint, cosmetics, and other industries as pigments. Surface characteristics of these minerals have been studied extensively both in resource recovery by flotation and in the preparation of colloidal dispersions. In this current research, the wetting characteristics of goethite (FeOOH) and hematite (Fe_2O_3) have been analyzed by means of contact angle, bubble attachment time, and Atomic Force Microscopy (AFM) measurements as well as by Molecular Dynamics Simulation (MDS). Goethite is naturally hydroxylated and wetted by water at all pH values. In contrast, the anhydrous hematite surface (001) was found to be slightly hydrophobic at natural pH values with a contact angle of about 50°. At alkaline pH hydroxylation of the hematite surface occurs rapidly and the hematite becomes hydrophilic. The wetting characteristics of the hematite surface then vary between the hydrophobic anhydrous hematite and the completely hydrophilic hydroxylated hematite, similar to goethite. The hydrophobicity can be restored by heating of the hydroxylated hematite surface at 60 °C. The hydrophobic character of the anhydrous hematite (001) surface is confirmed by MDS which also reveals that after hydrolysis the hematite (001) surface can be wetted by water, similar to the goethite (001) surface.

1. Introduction

Iron oxide minerals are among the most abundant minerals in the earth's crust. Commonly available iron oxide minerals are magnetite (Fe_3O_4), hematite (Fe_2O_3), goethite (FeOOH), limonite

* Corresponding author.
E-mail addresses: kaustubh.shrimali@gmail.com (K. Shrimali), jiaqi.jin90@gmail.com (J. Jin), behzadvaziri@hotmail.com (B.V. Hassas), X.Wang@utah.edu (X. Wang), Jan.Miller@utah.edu (J.D. Miller).

http://dx.doi.org/10.1016/j.jcis.2016.05.030
0021-9797/

($FeOOH{\cdot}nH_2O$) and siderite ($FeCO_3$). Magnetic separation is most frequently used for the processing of iron ores containing magnetite. However, flotation is used for most hematite/goethite ores requiring concentration to satisfy specifications for pelletization. Reverse flotation of silica from hematite is by far the most common route for the processing of iron ore containing silica gangue [1]. In reverse flotation of iron ore, quartz, the major impurity, is floated using ether amines and the iron oxide minerals are depressed, typically using polysaccharides such as starch, with the process carried out at pH 10.5. It is usually effective for feed varying from 10 μm to 150 μm in particle size. In Brazil more than 300 million tons of iron ore concentrate production per annum is achieved using polysaccharides in the reverse flotation process to remove silica gangue, while in the US the production is about 40 million tons annually.

According to authors' best knowledge, measurement of captive bubble contact angles for a natural hematite crystal have not been reported, but contact angle measurements on iron ore samples containing varying amounts of hematite, goethite, clay and quartz have been reported using the capillary method [2]. Even the effect of pH on the wettability of hematite and goethite has not been reported in the literature. Hydroxylation of the hematite surface at alkaline pH values has not been reported either, though it is reported that goethite is the thermodynamically stable form of ferric oxide in water [3].

In the present work, contact angle measurements were performed at different pH values for hematite and goethite to reveal the effect of pH on wettability. Molecular Dynamics Simulation (MDS) has been used to determine water sessile drop contact angles at various mineral surfaces [4] and was used in this research to determine contact angles for hematite, goethite and hydroxylated hematite surfaces. These contact angle measurements for hematite were complemented by bubble attachment time measurements. Atomic Force Microscopy (AFM) has been used extensively for surface force measurements [5–14], and in this work the wettability of hematite was also examined with in-situ surface force measurements at the hematite surface for different pH values. In these surface force measurements hematite particles were used as a colloidal probe and surface forces were measured between the hematite colloidal probe and the 001 hematite surface. This method is being reported for the first time.

Due to the marked increase in computational capabilities in recent years, MDS can be used to explore water/mineral interactions at the molecular-level [15,16]. Compared to quantum mechanical calculations, MDS has a greater capacity for studying a system with a large number of atoms. Because of this remarkable ability to simulate large systems, the contact angle of water nanodrops at solid surfaces can be determined by MDS [17]. In this study, MDS contact angles of the hematite (001) surface, the hydroxylated hematite (001) surface, and the goethite (001) surface were determined and the results compared to the experimental measurements.

The significance of the results is important in the understanding of existing flotation processes and in the design of new flotation separations [18]. In addition to the significance of these findings in the field of flotation chemistry, the results being reported are important to the pigment industry, since dispersion of hematite pigments will be influenced significantly by the wetting characteristics of hematite. Pigment powders used in the paint industry have to be properly dispersed in the aqueous solution, as dispersion of the suspension determines the quality of the paint. The final paint should be stable on storage and should not agglomerate or aggregate. Other applications include the preparation of composites and cosmetic products.

2. Experimental

2.1. Minerals and reagents

The specular hematite crystals for contact angle measurements and AFM surface force measurements were obtained from "The Iron Quadrangle," Brazil. The quality of the high purity single crystals was confirmed by XRD and EDAX analysis. Presence of peaks at 2θ angles of 84.48° and 39.26° signify that the crystal surface represents the (001) plane of hematite as described in the literature [19]. The (001) crystal surface of hematite was polished with a nylon polishing cloth purchased from Buehler using a DiaDuo-2 water based 1-μm diamond suspension obtained from Struers (Ballerup, Denmark). Natural smooth crystals obtained from the same source were used for AFM force measurements. The rms roughness of the 001 crystal surface used for force measurements was found to be around 2.69 nm.

Pulverized hematite samples used for bubble attachment time measurements were obtained from Orrisa, India, and the particle size used for bubble attachment time measurements was 106 × 75 μm.

Samples for zeta potential measurements were obtained by crushing and pulverizing the Brazilian crystals and the particle size used was minus 65 μm. Dry as well as wet screening was done to obtain the samples of 106 × 75 μm for bubble attachment time measurements and minus 65 μm for zeta potential measurements.

The goethite "needle ore" crystal sample used for contact angle measurements was obtained from Cary Mine, Ironwood, Gogebic County, Michigan. The crystal was polished by the same method used for hematite. The ground goethite samples for bubble attachment time measurements and zeta potential measurements were obtained by crushing and pulverization. The quality of the crystals was confirmed by XRD and EDAX analysis.

Sodium hydroxide (NaOH) and hydrochloric acid (HCl) obtained from Sigma-Aldrich were used to adjust the pH. Potassium chloride (KCl), also obtained from Sigma-Aldrich, was used as the electrolyte background in force measurements. DI water was obtained from a Millipore system in the laboratory with specific conductance of 18 MΩ cm.

2.2. Captive bubble contact angle

Both hematite and goethite samples were cleaned with acetone, ethanol, ample amounts of DI water and dried with ultra-pure nitrogen before measurements. The hematite sample was oven dried at 60 °C for 25 min and then cooled for half an hour open to the atmosphere before each contact angle measurement. The distance between the needle and the sample was kept constant for each captive bubble contact angle measurement. All the measurements were done in 0.001 M KCl solution and pH was adjusted by adding the desired amount of HCl or NaOH solution. Before every contact angle measurement, the sample was conditioned in respective pH solutions for 15 min and measurement was done in the same solution. At least 20 contact angle measurements were obtained for each pH at different locations and they were averaged to obtain the reported contact angle value for each pH. Variation in contact angle measurements was ±10°.

2.3. Bubble attachment time measurements

Bubble attachment time measurements were done using an MCT 100 electronic induction timer instrument. The particle bed was prepared in a cuvette of 1 cm × 1 cm × 2 cm and the particles were conditioned for 20 min in the same vial before taking each

reading. Each experiment was conducted with a constant bubble diameter of 1 mm with a constant gap between the bubble and particle bed. Ten runs were performed for each condition, and the number of successful attachments was reported as an attachment ratio. To qualify as a successful attachment, the system was tapped gently to assure that attachment had occurred by film rupture and displacement. Further details on the method are given elsewhere [20–22].

2.4. Zeta potential measurements

The electrophoresis method was used for zeta potential measurements for goethite and hematite particles and was performed as a function of pH using PALS Zeta Potential Analyzer from Brookhaven Instrument Corp. For each experiment 80 mg of goethite and hematite samples of respective sizes were added to 80 ml of 0.001 M KCl solution in a beaker and the mixture was allowed to stir for 30 min. From the beaker, while stirring, 10 ml of suspension was transferred to each of 8 vials using a pipette. Solutions of 0.1 M HCl and 0.1 M NaOH were used to adjust the pH of the suspensions. Every vial was kept in the shaker at a speed of 250 RPM for another 15 min before taking electrophoretic mobility measurements. At least 20 measurements were done and the average value reported.

2.5. Atomic force measurements

The AFM system used for surface force measurements was a Nanoscope V controller, a PF scanner from Veeco and a liquid cell obtained from Bruker Corporation, Santa Barbara, CA. The colloidal probe technique was used for surface force measurements. Tipless silicon cantilevers were obtained from Mikromasch. Hematite particles of around 15 μm in size were picked using a clean tungsten wire attached to a micromanipulator. The hematite particle was attached at the apex of the cantilever using "Norland Optical Adhesive." The adhesive was also applied at the apex of the cantilever using the tungsten wire, before attaching the hematite particle. The adhesive was then hardened by keeping it under a UV source. Two different colloidal probes were prepared with two different configurations of the hematite particle on the cantilever. In one case, the hematite probe particle was glued in a way that contact would be with the (001) crystal face, while in the other case the hematite probe particle was oriented so that the (100) crystal surface would contact the surface as shown in Fig. 1.

Scanning electron microscopy was used to make sure that there was no contamination of glue on the attached hematite probe particle surface. The hematite probe particle size was also measured from the scanning electron microscope image. Both particles had an approximate size of 15 μm. The spring constant for the cantilever was measured using the thermal tune method provided with the instrument and was used for data analysis. In order to measure the surface forces between the flat hematite crystal (001) surface and the hematite probe particle, both probes as well as the crystal surface were cleaned by the procedure described in previous sections. In order to prevent any possible degradation of glue, the probe was oven dried at 40 °C for 2 h. Measurements were performed in 0.001 M KCl solution with varying pH values. Before each force measurement, 25 μm^2 of surface was imaged in contact mode in order to determine the surface-probe interaction. Desired flat surface positions were then selected for force measurements where at least 5 force measurements were conducted for each point. One of the representative points was picked and the average value of the 5 measurements was calculated for subsequent analysis. The raw data were analyzed using "Scanning Probe Image Processor (SPIP)" software which converted the deflection curves to force curves. The hematite crystal and probe were immersed in the specified pH solution in the liquid cell for at least 20 min for equilibration of the system before any imaging or force measurements were made.

In order to correlate force curves between the hematite crystal (001) surface and the hematite probe with a reference, force measurements at the hematite crystal (001) surface were also performed using a Diamond-Like Carbon (DLC) tip, which is naturally hydrophobic. The DLC cantilevers were obtained from Budget Sensors, sold under the name "ContDLC." The point of zero charge for DLC tips has been reported to be at pH ~ 4 [23].

2.6. Molecular dynamics simulation

Amber, an MDS program, was used to simulate water drop spreading at the hematite (001) and goethite (001) surfaces. In the Amber program, this total energy is expected to include the Coulombic (electrostatic) interactions, the short-range interactions (van der Waals energy term), and the bonded interactions. The bonded terms include the bond stretch and angle bend energy terms that are represented in the water models as harmonic terms. The Coulombic energy is represented by Eq. (1) in which the energy of the interaction is inversely proportional to the distance of separation r_{ij}. The terms q_i and q_j are partial charges for atoms i and j. The term e is the charge of an electron, and ϵ_0 is the dielectric permittivity of a vacuum (8.85419×10^{-12} F/m).

$$E_{Coulombic} = \frac{e^2}{4\pi\epsilon_0} \sum_{i \neq j} \frac{q_i q_j}{r_{ij}} \quad (1)$$

The van der Waals energy term, represented by the conventional Lennard-Jones (12-6) function, includes the short-range repulsion associated with the increase in energy as two atoms

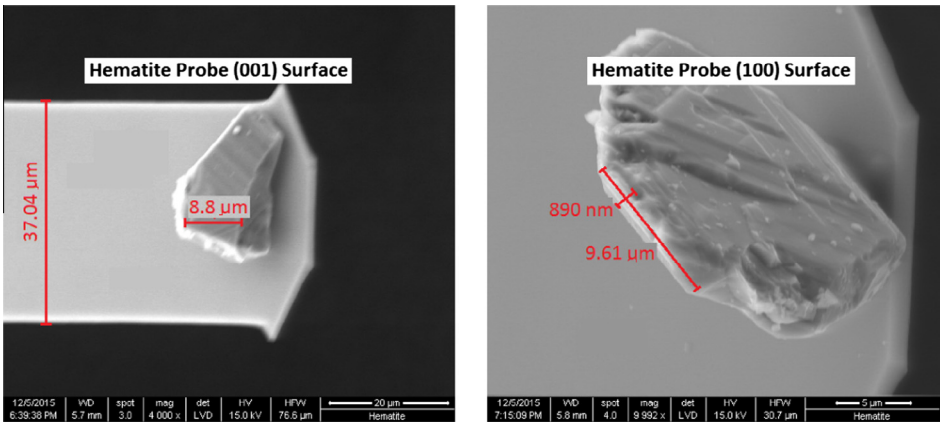

Fig. 1. SEM micrographs of hematite colloidal probes showing 001 and 100 surfaces.

approach each other and the attractive dispersion energy. The term ε_{ij} is the depth of the potential well, and $r_{m,ij}$ is the distance at which the potential reaches its minimum.

$$E_{VDW} = \sum_{i \neq j} \varepsilon_{ij} \left[\left(\frac{r_{m,ij}}{r_{ij}} \right)^{12} - \left(\frac{r_{m,ij}}{r_{ij}} \right)^{6} \right] \quad (2)$$

The interaction parameters between unlike atoms are calculated according to the arithmetic mean rule for the distance parameter, r_m, and the geometric mean rule for the energy parameter, ε:

$$r_{m,ij} = \frac{1}{2(r_{m,i} + r_{m,j})} \quad (3)$$

$$\varepsilon_{ij} = \sqrt{\varepsilon_i \varepsilon_j} \quad (4)$$

The rigid SPC/E water model has the closest average configurational energy to the experimental value (−41.5 kJ mol^{-1}) [24,25]. Thus, we selected the SPC/E water model for exploring the sessile drop wettability of the hematite (001) and goethite (001) surfaces. The Lennard-Jones parameters r_m, ε and atomic partial charge q for the Fe, O, and H atoms of the hematite and goethite crystals are from CLAYFF [26].

To measure the MDS sessile drop contact angle of water at the hematite (001) and goethite (001) surfaces, a water drop containing 1270 water molecules was put on the surface at the bottom of a simulation periodic box. According to a previous MDS study [4], in the size range from 850 to 1700 water molecules, drop size doesn't have much effect on the sessile drop contact angle determined by MDS. In order to remove the periodic images of the drop in measuring the simulated contact angle, the surface needed to have sufficient area. In our study, the horizontal extent of the hematite (001) and goethite (001) surfaces used for simulated contact angles was about 150 Å × 150 Å. These large surfaces were built based on the lattice parameters from the American Mineralogist Crystal Structure Database [27]. A previous Scanning Tunneling Microscope (STM) study revealed that iron atoms were not found at the hematite (001) surface [28]. Thus, in the MD simulations, the hematite (001) surface was reconstructed to mimic the STM experimental observation.

A relatively small hydroxylated hematite (001) surface unit (10 Å × 10 Å) was prepared by quantum chemical calculation using the QUICKSTEP module of the CP2K packages. The input was a water molecule on top of the hematite (001) surface. After energy minimization, the water molecule reacted with the iron and oxygen atoms at the hematite (001) surface and produced two hydroxide anions, i.e. hydrolysis of the hematite (001) surface. Then the 10 Å × 10 Å unit of the hydroxylated hematite (001) surface was expanded to prepare the large surface for MDS contact angle measurement. The vertical extent of the periodic simulation boxes was set at 150 Å to avoid the influence of periodic conditions on the water drops. One water molecule in this periodic volume of about 3.0×10^6 Å^3 would provide a saturated atmosphere, so the water drop is stable under these conditions.

Because of the large number of atoms (about 50,000) in these simulations, we used a total simulation time of 1 ns (1×10^6 steps each of 1 fs), including a 500 ps equilibration period and another 500 ps analysis period. The contact angles were measured on an average for the second 500 ps. The canonical ensemble (NVT) was used for the MD simulations of interfacial water molecules at the selected mineral surfaces, in which case the amount (N), volume (V) and temperature (T) are conserved. The simulation temperature was set as 298 K.

2.7. Scanning electron microscopy

A Hitachi S-4800 high resolution field emission scanning electron microscope was used to analyze the hematite probe. Comparing the crystal structure of the hematite and the probes used for force measurements it is expected that one probe represents the (001) crystal face of hematite and the other probe represents the (100) face of hematite. As expected, the surface of the hematite crystal was found to be the (001) surface as established by X-ray diffraction results. The horizontal as well as vertical images of the tip suggest that there is no contamination from glue on the hematite colloidal probe particle.

3. Results and discussion

Oxide minerals are generally thought to be hydrophilic and well wetted by water. However, complete wetting, as shown from recent studies, depends on hydroxylation of the mineral surface in order to provide H-bonding sites for interfacial water molecules. In some cases, it seems that hydroxylation is rapid and the oxide surfaces are wetted by water within minutes. In other cases, the reaction with water is slow and the time for hydroxylation/wetting is extended to days [29,30].

3.1. Captive bubble contact angle

Contact angle measurements for the specular hematite and goethite surfaces were done in 0.001 M KCL solutions at different pH values. The (001) surface of hematite was found to be naturally hydrophobic with a captive bubble contact angle of about 50° at natural pH, as shown in Fig. 2. Experimental results also suggest that hematite remains hydrophobic at acidic pH values but becomes strongly hydrophilic at basic pH values with an experimental contact angle of 0° (Fig. 2). It is observed that hematite loses its hydrophobicity when kept at basic pH apparently due to hydroxylation of the surface. It should be noted that slow hydroxylation of the hematite surface takes place even at natural pH with the contact angle being reduced to about 20° within 24 h. Goethite, which is representative of the fully hydroxylated state of hematite, has an experimental contact angle of 0° at all pH values (Fig. 2). Hydroxylation of the hematite surface is expected because at basic pH, goethite is thermodynamically more stable than hematite. It is observed that hydroxylation of the hematite surface is reversible and the initial hydrophobic state can be achieved. The reversibility of the hydroxylation reaction was examined. After measuring the contact angles on hematite at pH 11 and transferring the sample to another solution of pH 5.3 for another measurement, the hematite sample still showed a contact angle of 0°. The, hematite achieved its initial hydrophobic state after washing and heating for 25 min at 60°. The results show that the initial hydrophobic state for the (001) crystal surface of hematite at pH 5.3 can be restored and that the surface hydrolysis reaction is reversible.

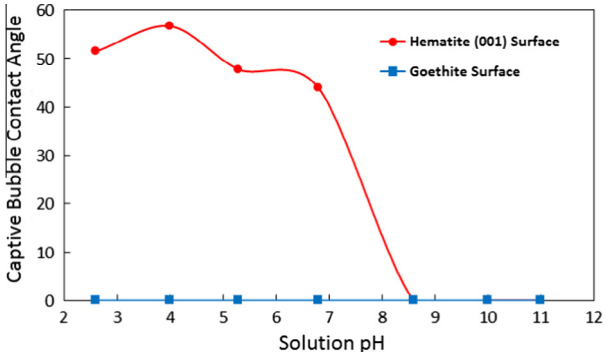

Fig. 2. Captive bubble contact angle for the (001) specular hematite surface and goethite surface with variation of solution pH (0.001 M KCl).

3.2. Sessile drop MDS contact angle results

As mentioned in the experimental section, the hematite (001) surface can be organized to conform to a surface state revealed by STM results reported in the literature [28]. Thus, the hematite (001) surface consists of exposed oxygen atoms. Quantum calculations using the QUICKSTEP module of the CP2K packages confirm that the re-organized hematite (001) surface (oxygen atoms exposed) is stable with lower energy than the ideal hematite (001) surface (iron atoms exposed).

Snapshots of the nanoscale water drop spreading at the hematite (001) surface, hydroxylated hematite (001) surface, and goethite (001) surface are shown in Fig. 3. MDS sessile drop contact angles of the selected surfaces are listed in Table 1. MDS analysis of this re-organized hematite surface confirms the hydrophobic state in accordance with the experimental captive bubble contact angle measurements. The water drop spreads very well at the hydroxylated hematite surface and at the goethite surface, which is also consistent with experimental results. The hydroxide groups at the hydroxylated hematite surface and at the goethite surface are hydrogen bonding accepters or donors. The interfacial water molecules should have strong interactions, such as hydrogen bonding, with the hematite (001) surface and goethite (001) surface. As

Table 1
MDS sessile drop contact angles for the reorganized anhydrous hematite (001) surface, hydroxylated hematite (001) surface, and the goethite (001) surface.

Mineral surface	Chemical formula	MDS contact angle (deg)
Hematite (001) surface	Fe_2O_3	60
Hydroxylated hematite (001) surface	Bulk: Fe_2O_3 Surface: FeOOH	10
Goethite (001) surface	FeOOH	10

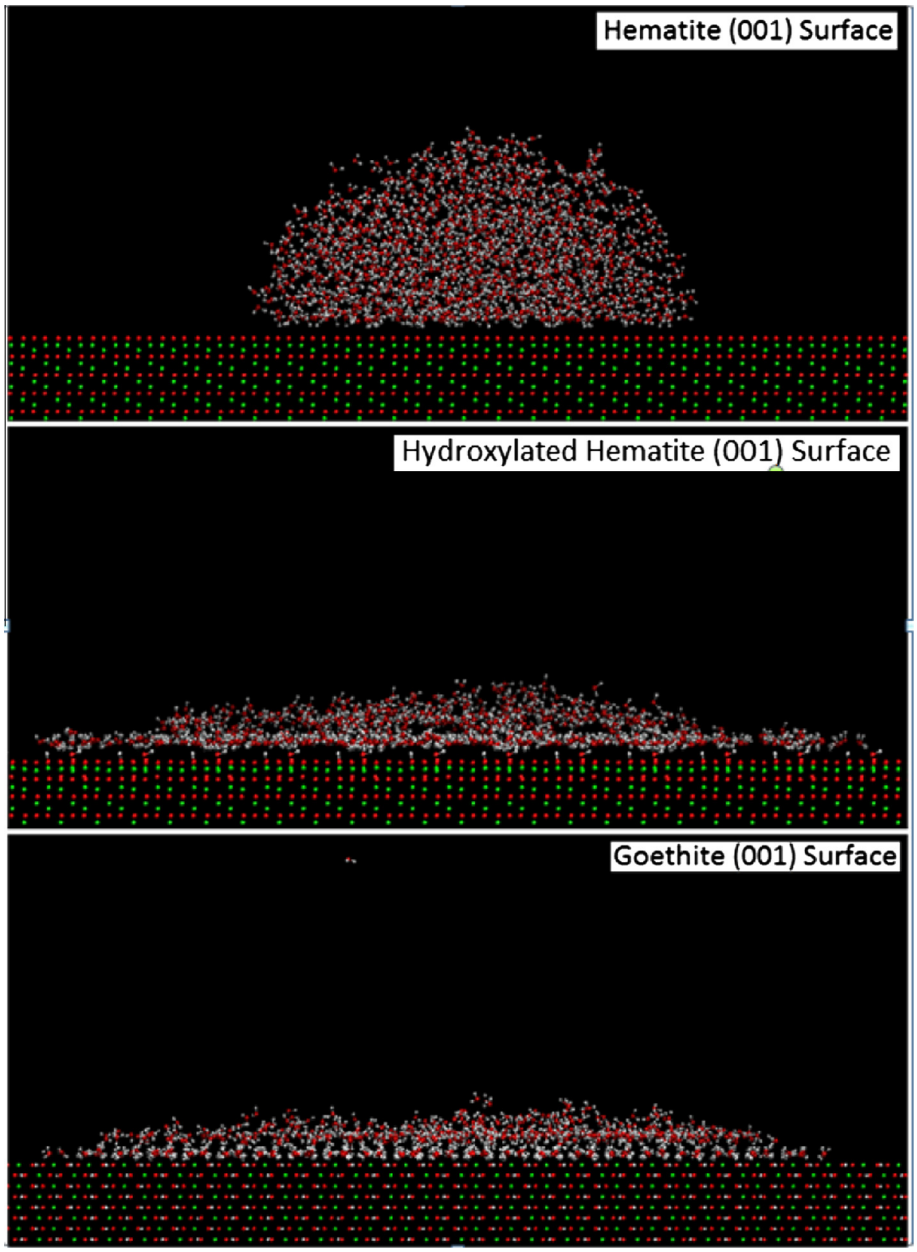

Fig. 3. Snapshot of a water drop containing 1270 water molecules spreading at the reorganized anhydrous hematite (001) surface (top), hydroxylated hematite (001) surface (middle), and the goethite (001) surface (bottom). The simulation time is 0.5 ns. The atoms' color code is as follows: green, Fe; red, O; white, H.

a result, the hematite surface and goethite surface can be wetted by water. On the other hand, the oxygen atoms exposed at the reorganized hematite (001) surface in the absence of hydroxylation have covalent bonds with the iron atoms from the bulk crystal and have been satisfied, so there are no hydrogen bonding accepters or donors at the reorganized anhydrous hematite surface. Similar phenomena have been observed for other systems such as talc and kaolinite [16,31]. Future MDS study of the interfacial water structures at the reorganized anhydrous hematite (001) surface, the hydroxylated hematite (001) surface, and the goethite (001) surface will provide further molecular-level information.

3.3. Bubble attachment time measurements

Qualitative analysis of bubble attachment time measurements for hematite particles of size 106 × 75 μm was done at different pH values in 0.001 M KCl solutions. Bubble attachment time for hematite particles at pH 5.5 was 40 ms and no attachment took place at pH 10.5. The contact time of the bubble with the particle bed varied from 10 ms to 150 ms for all cases.

3.4. Zeta potential measurements

The electrophoresis technique was used to measure the zeta potential for hematite as well as for goethite. The point of zero charge (PZC) for hematite was found to be ~pH 6.2 and for goethite the PZC was found to be ~pH 5 (Fig. 4). These PZC values for natural hematite and goethite agree well with values reported in the literature [32,33]. These values suggest that charging hematite or goethite surfaces doesn't have a significant effect on the contact angle. At pH 4 the positively charged hematite has a captive bubble contact angle of 51° whereas goethite has a contact angle of 0° at pH 5.5, approximately the point of zero charge for goethite.

3.5. AFM surface force measurements

Results from surface force measurements between the hematite probes (both orientations) and the hematite crystal (001) surface at different pH values are presented in this section to further understand the surface characteristics of hematite. Two different colloidal probes were prepared with two different orientations of the hematite particle on the cantilever. One of the particles was glued in a way that the hematite particle could touch the surface with its (001) crystal face, while the other colloidal probe hematite particle approached the hematite crystal (001) surface with the (100) surface as shown earlier in the experimental section (Fig. 1). Hence, in one case we expect that force measurements are between the hematite crystal (001) surface and the hematite probe (001) surface. In the other case we expect that force measurements are between the hematite crystal (001) surface and the hematite probe (100) surface. The hematite crystal used for AFM force measurements had an rms roughness of 2.69 nm.

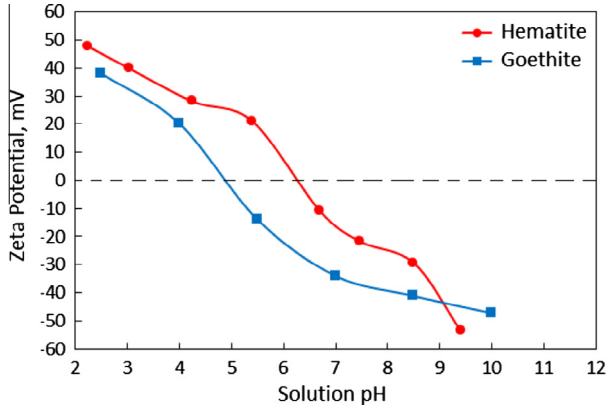

Fig. 4. Zeta potential variation of hematite and goethite with solution pH in 0.001 M KCl.

Force curves between the hematite probe (001) and the hematite crystal (001) surface (Fig. 5a and b) are presented with measurements done at pH 2.7 and 5.5 in 0.001 M KCl solution. The curves show the sudden occurrence of an attractive force at a distance of around 40–50 nm. This attraction is much stronger and of longer range than van der Waals forces alone, which are much weaker and not long range forces. Hence, we conclude the presence of the hydrophobic force at this pH, confirming that hematite is slightly hydrophobic at these pH values as has been suggested by contact angle and bubble attachment time measurements as well as MDS results. These attractive forces may be due to the presence of nano bubbles present at such hydrophobic surfaces. As suggested in the literature, when two hydrophobic surfaces are brought close to each other, capillary bridging between these nano bubbles takes place leading to attraction which can be considered to be an explanation for hydrophobic interactions [34–41]. One more observation that can be made from Fig. 5a and b is the occurrence of a slight repulsive force just before a stronger attractive force is observed. It is expected that this repulsive force is the consequence of compression of the nano bubbles taking place just before the drainage/bridging coalescence occurs which leads to attractive forces. Similar kinds of attractive forces were observed in the case of force curves obtained between the hematite probe (100) and the hematite crystal (001) surface (Fig. 5a and b). Double layer repulsive forces at these distances cannot be ignored but they are greatly overshadowed by stronger attractive hydrophobic forces. Variability in the distance of the attractive forces is expected as different positions on the surface will have different sizes and occurrence of nano bubbles [34].

Force curves between the hematite probe (001) and the hematite crystal (001) surface are presented in Fig. 5c with measurements done at pH 10.5. Occurrence of just repulsive forces in this case suggests that there is no bridging of nano bubbles. This indicates that at alkaline pH, hydroxylation of the hematite surface occurs rapidly and the hematite becomes hydrophilic. Similar results were obtained from force curves between the hematite probe (100) and the hematite crystal (001) surface, confirming the contact angle results from experimental measurements and MDS simulations (Fig. 5c).

As suggested earlier, hydroxylation of the hematite surface is reversible and the initial hydrophobic state can be restored by washing and heating the sample in an oven at 60° for 25 min, which apparently dehydrates the surface. This observation was also confirmed by performing two sets of experiments. First, force measurements were performed between the hematite probe and the hematite crystal (001) surface at pH 5.5, just after the sample was removed from the 0.001 M KCl (pH 10.5) with conditioning time being 20 min before removal. The second experiment was performed between the hematite probe and the crystal surface at pH 5.5 after removal from 20 min conditioning of 0.001 KCl (pH 10.5), washing them as described previously, and heating them as before. The first experiment showed a repulsive force (Fig. 5d) weaker than that obtained in the case of force measurements done at pH 10.5. The repulsive force in this case was not as repulsive as was obtained in Fig. 5c. This suggests that the hematite retains some hydrophilicity at natural pH even after it is removed from the alkaline pH solution. Under these conditions it appears that partial restoration of the anhydrous hematite surface is achieved. The second set of force measurement experiments, in which the hematite crystal (001) surface as well as the probes were washed and heated after being kept in alkaline solution, showed attractive

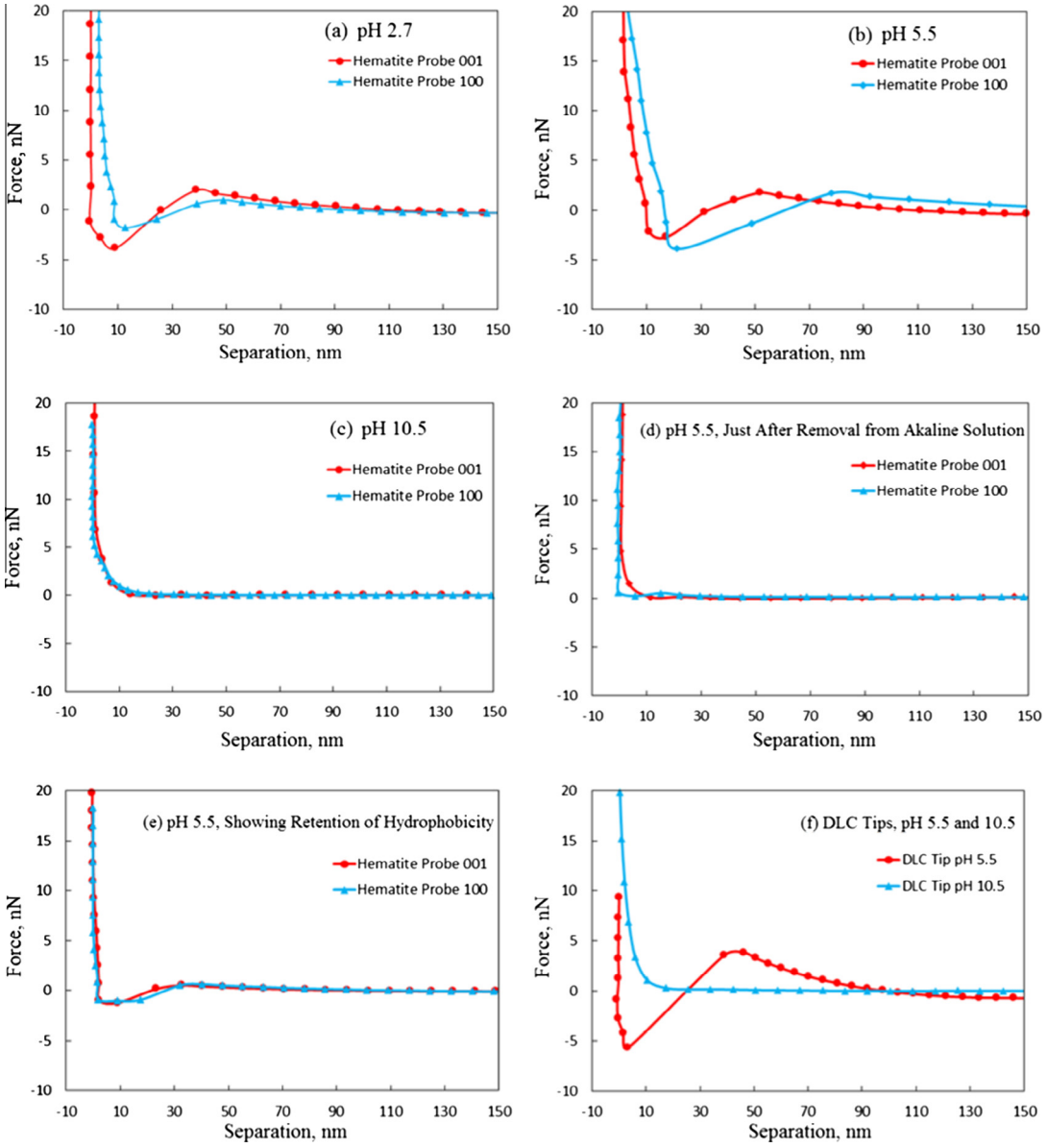

Fig. 5. (a) Force curve showing attraction for hematite probes (001 and 100) and hematite crystal (001) surface at pH 2.7. (b) Force curve showing attraction for hematite probes (001 and 100) and hematite crystal (001) surface at pH 5.5. (c) Force curve showing repulsion for hematite probes (001 and 100) and hematite crystal (001) surface at pH 10.5. (d) Force curve showing repulsion for hematite probes (001 and 100) and hematite crystal (001) surface at pH 5.5 just after removal from alkaline medium indicating that hematite restores the hydrophilicity even after removal from alkaline pH. (e) Force curve showing attraction for hematite probes (001 and 100) and hematite crystal (001) surface at pH 5.5 after removal from alkaline medium and heating indicating that the initial surface state of hematite could be restored by heating. (f) Force curve showing forces between the hydrophobic DLC tip and the hematite crystal (001) surface at pH 5.5 and 10.5.

forces (Fig. 5e) at a 40–50 nm separation distance similar to that obtained when force measurements were done at pH 5.5 and 2.7. These results suggest that the hydroxylation reaction is reversible and the initial surface state can be restored by washing and heating, which apparently dehydroxylates the surface.

The variation in polarity and the degree of hydrophobicity of the hematite crystal (001) surface was also confirmed by doing force measurements using a hydrophobic Diamond-Like Carbon (DLC) tip. The charging behavior of the DLC tip was found to have an iso electronic point at pH 4 [23]. AFM force measurements done at pH 5.5 between the DLC tip and the hematite crystal (001) surface showed a strong long range attractive force (Fig. 5f) similar to that obtained during force measurements between the hematite probe and the hematite crystal (001) surface. These results support the hematite probe measurements and analysis. Similar AFM force measurements were performed between the DLC tip and the hematite crystal (001) surface at pH 10.5 (Fig. 5f). The repulsive forces observed demonstrate that the (001) hematite surface is no longer hydrophobic in alkaline solution and that hydroxylation of the hematite surface takes place under these conditions.

4. Summary and conclusions

Our results have provided important information not previously reported and define conditions for wetting of the hematite surface. Improved understanding of the wetting characteristics of hematite has been contributed. First, the research demonstrates the utility of MDS and AFM in the wetting analysis of hematite surfaces. Second, the significance of hydroxylation in the wetting of the hematite

surface has been established. Third, sensitivity to pH and hydration/hydroxylation time has been described for hematite with respect to reversibility and the sensitive nature of the hydrophobic/hydrophilic balance of the hematite surface state.

The AFM colloidal probe technique for surface force measurements has been used to help explain the wetting characteristics of hematite and represents a unique application of AFM for advances in colloid chemistry.

In conclusion, results from this research have helped to describe the surface properties of hematite. It has been found that the (001) hematite surface is hydrophobic at natural pH ($\theta = 50^\circ$) but immediately becomes hydrophilic and is well wetted in alkaline solution ($\theta = 0^\circ$) due to a surface hydroxylation reaction.

Nanoscale MDS sessile drop contact angles confirm the experimental captive bubble contact angle measurements. The lack of H bonding of interfacial water molecules at the anhydrous (001) hematite surface accounts for its hydrophobicity. In contrast, relatively strong H bonding interactions between the interfacial water molecules and both the hydroxylated hematite (001) surface and the goethite (001) surface account for their hydrophilic character. Based on zeta potential measurements, the charging behavior of hematite and goethite has little effect on the wetting characteristics of the surfaces.

AFM results also demonstrate the same trend as experimental captive bubble contact angle measurements. Strong long range attractive hydrophobic forces at pH 5.5 and pH 2.7 reveal that the surface is hydrophobic at acidic and natural pH values. In contrast, presence of only repulsive forces at alkaline pH values suggests that surface hydroxylation takes place at this pH making the surface hydrophilic and well wetted by water.

Evidence has been provided indicating that hematite retains its hydrophilicity even after removal from the alkaline medium, and that the initial hydrophobic surface state could only be restored by drying at a modest temperature which leads to dehydroxylation of the surface.

These results are of significant importance to the mining, pigment, paint and battery industries.

In reverse flotation of iron ore, quartz, the major impurity, is floated using ether amines and the iron oxide minerals are depressed, typically using polysaccharides such as starch. Reverse flotation of iron ore is usually carried out at pH 10.5. In this regard, the role of polysaccharides in reverse flotation is considered since hematite is already hydrophilic at the alkaline pH in which reverse flotation is usually carried out. This surface chemistry study is a step forward in understanding reverse flotation in the processing of iron ore [42–44]. In view of the results from the current research, it seems that the purpose of polysaccharides is to prevent amine adsorption by hematite and its flotation with quartz. In this regard, further study of the competitive adsorption between polysaccharides and amines at the hematite surface is planned.

The surface properties of hematite established in our paper can help in deriving better chemistry for dispersion of hematite based pigments at different pH values [45,46]. Such wetting information could be of significant importance in the preparation of certain solid state electrolytes/electrodes for the development of advanced battery technology [47,48].

Acknowledgements

This work was funded by the Division of Chemical Sciences, Geosciences, and Biosciences, Office of Basic Energy Sciences of the U.S. Department of Basic Energy through Grant No. DE-FG03-93ER14315. We want to thank Dr. Shivakumar Angadi for research assistance and providing the hematite samples from Orissa, India. Thanks to Mr. Venkata Atluri for help with the research. Also we want to thank Professor P.R.G. Brandao for hematite samples from Brazil and the information which initiated this research. Finally, we thank Ms. Dorrie Spurlock for her assistance in the preparation of the manuscript.

References

[1] D. Mowla, G. Karimi, K. Ostadnezhad, Removal of hematite from silica sand ore by reverse flotation technique, Sep. Purif. Technol. 58 (3) (2008) 419–423.
[2] S.M. Iveson, S. Holt, S. Biggs, Advancing contact angle of iron ores as a function of their hematite and goethite content: implications for pelletising and sintering, Int. J. Miner. Process. 74 (2004) 281–287.
[3] I. Diakonov, I. Khodakovsky, J. Schott, E. Sergeeva, Thermodynamic properties of iron oxides and hydroxides. I. Surface and bulk thermodynamic properties of goethite (α-FeOOH) up to 500 K, Eur. J. Mineral. 6 (6) (2004) 967–984.
[4] J. Jin, J.D. Miller, L.X. Dang, C.D. Wick, Effect of surface oxidation on interfacial water structure at a pyrite (1 0 0) surface as studied by molecular dynamics simulation, Int. J. Miner. Process. 139 (2015) 64–76.
[5] G. Binnig, C. Gerber, E. Stoll, T.R. Albrecht, C.F. Quate, Atomic resolution with atomic force microscope, EPL (Europhys. Lett.) 3 (12) (1987) 1281.
[6] N.A. Burnham, R.J. Colton, Measuring the nanomechanical properties and surface forces of materials using an atomic force microscope, J. Vac. Sci. Technol., A 7 (4) (1989) 2906–2913.
[7] F.J. Giessibl, Advances in atomic force microscopy, Rev. Mod. Phys. 75 (3) (2003) 949.
[8] I. Larson, C.J. Drummond, D. Chan, F. Grieser, Direct force measurements between silica and alumina, Langmuir 13 (7) (1997) 2109–2112.
[9] A.C. Hillier, S. Kim, A.J. Bard, Measurement of double-layer forces at the electrode/electrolyte interface using the atomic force microscope: potential and anion dependent interactions, J. Phys. Chem. 100 (48) (1996) 18808–18817.
[10] G. Toikka, R.A. Hayes, Direct measurement of colloidal forces between mica and silica in aqueous electrolyte, J. Colloid Interface Sci. 191 (1) (1997) 102–109.
[11] W.A. Ducker, T.J. Senden, R.M. Pashley, Direct measurement of colloidal forces using an atomic force microscope, Nature 353 (6341) (1991) 239–241.
[12] R.G. Miller, P.J. Bryant, Atomic force microscopy of layered compounds, J. Vac. Sci. Technol., A 7 (4) (1989) 2879–2881.
[13] J. Liu, L. Sandaklie-Nikolova, X. Wang, J.D. Miller, Surface force measurements at kaolinite edge surfaces using atomic force microscopy, J. Colloid Interface Sci. 420 (2014) 35–40.
[14] J. Liu, J.D. Miller, X. Yin, V. Gupta, X. Wang, Influence of ionic strength on the surface charge and interaction of layered silicate particles, J. Colloid Interface Sci. 432 (2014) 270–277.
[15] J. Jin, J.D. Miller, L.X. Dang, Molecular dynamics simulation and analysis of interfacial water at selected sulfide mineral surfaces under anaerobic conditions, Int. J. Miner. Process. 128 (2014) 55–67.
[16] H. Du, J.D. Miller, A molecular dynamics simulation study of water structure and adsorption states at talc surfaces, Int. J. Miner. Process. 84 (2007) 172–184.
[17] T. Werder, J.H. Walther, R. Jaffe, T. Halicioglu, P. Koumoutsakos, On the water–carbon interaction for use in molecular dynamics simulations of graphite and carbon nanotubes, J. Phys. Chem. B 107 (2003) 1345–1352.
[18] K. Shrimali, J.D. Miller, Polysaccharide depressants for the reverse flotation of iron ore, Trans. Indian Inst. Met. 69 (1) (2016) 83–95.
[19] R.L. Blake, R.E. Hessevick, T. Zoltai, L.W. Finger, Refinement of the hematite structure, Am. Mineral. 51 (1966) 123–129.
[20] B. Albijanic, O. Ozdemir, A.V. Nguyen, D. Bradshaw, A review of induction and attachment times of wetting thin film between air bubbles and particles and its relevance in the separation of particles by flotation, Adv. Colloid Interface Sci. 159 (2010) 1–21.
[21] Y. Ye, J.D. Miller, Bubble/particle contact time in the analysis of coal flotation, Coal Prep. 5 (1988) 147–166.
[22] Y. Ye, J.D. Miller, The significance of bubble/particle contact time during collision in the analysis of flotation phenomena, Int. J. Miner. Process. 25 (1989) 199–219.
[23] X. Yin, J. Drelich, Surface charge microscopy: novel technique for mapping charge mosaic surfaces in electrolyte solutions, Langmuir 24 (2008) 8013–8020.
[24] P.G. Kusalik, I.M. Svishchev, The spatial structure in liquid water, Science 265 (1994) 1219–1221.
[25] M.W. Mahoney, W.L. Jorgensen, A five-site model for liquid water and the reproduction of the density anomaly by rigid, nonpolarizable potential functions, J. Chem. Phys. 112 (2000) 8910–8922.
[26] R.T. Cygan, J.J. Liang, A.G. Kalinichev, Molecular models of hydroxide, oxyhydroxide, and clay phases and the development of a general force field, J. Phys. Chem. B 108 (2004) 1255.
[27] R.T. Downs, M. Hall-Wallace, The American mineralogist crystal structure database, Am. Mineral. 88 (2003) 247–250.
[28] M.F. Hochella Jr., Mineral surfaces: their characterization and their physical and reactive nature, in: D.J. Vaughan, R.A.D. Pattrick (Eds.), Mineral Surfaces, Chapman and Hall, London, 1995, pp. 17–60.
[29] D.J. Wesolowski, J.O. Sofo, A.V. Bandura, Z. Zhang, E. Mamontov, M. Předota, N. Kumar, J.D. Kubicki, P.R.C. Kent, L. Vlcek, M.L. Machesky, P.A. Fenter, P.T. Cummings, L.M. Anovitz, A.A. Skelton, J. Rosenqvist, Comment on "Structure

and dynamics of liquid water on rutile TiO_2 (1 1 0)", Phys. Rev. B 85 (2012) 167401.
[30] J.D. Miller, X. Wang, J. Jin, K. Shrimali, Interfacial water structure and the wetting of mineral surfaces, Int. J. Miner. Process. (2016), http://dx.doi.org/10.1016/j.minpro.2016.02/004.
[31] X. Yin, V. Gupta, H. Du, X. Wang, J.D. Miller, Surface charge and wetting characteristics of layered silicate minerals, Adv. Colloid Interface Sci. 179–182 (2012) 43–50.
[32] S.E. O'Reilly, M.F. Hochella, PH-dependent surface charging and points of zero charge II. Update, Geochim. Cosmochim. Acta 67 (2003) 4471–4487.
[33] I. Iwasaki, S.R.B. Cooke, D.H. Harraway, H.S. Choi, Iron wash ore slimes-some mineralogical and flotation characteristics, AIME Trans. 233 (1962) 97.
[34] A. Carambassis, L.C. Jonker, P. Attard, M.W. Rutland, Forces measured between hydrophobic surfaces due to a submicroscopic bridging bubble, Phys. Rev. Lett. 80 (1998) 5357.
[35] V. Wallqvist, P.M. Claesson, A. Swerin, J. Schoelkopf, P.A.C. Gane, Interaction forces between talc and hydrophobic particles probed by AFM, Colloid Surf. A: Physicochem. 277 (2006) 183–190.
[36] A.V. Nguyen, J. Nalaskowski, J.D. Miller, H.J. Butt, Attraction between hydrophobic surfaces studied by atomic force microscopy, Int. J. Miner. Process. 72 (2003) 1–4.
[37] J. Drelich, J. Nalaskowski, A. Gosiewska, E. Beach, J.D. Miller, Long-range attractive forces and energy barriers in de-inking flotation: AFM studies of interactions between polyethylene and toner, J. Adhes. Sci. Technol. 14 (14) (2000) 1829–1843.
[38] S. Assemi, P.G. Hartley, P.J. Scales, R. Beckett, Investigation of adsorbed humic substance using atomic force microscopy, Colloid Surf. A: Physicochem. 248 (2006) 17.
[39] E. Pensini, B.E. Sleep, C.M. Yip, D.O. Carroll, Forces of interaction between fresh iron particles and iron oxide (magnetite): effect of water chemistry and polymer coatings, Colloid Surf. A: Physicochem. 433 (2013) 104–110.
[40] B. Vaziri Hassas, H. Caliskan, O. Guven, F. Karakas, M. Cinar, M.S. Celik, Effect of roughness and shape factor on flotation characteristics of glass beads, Colloid Surf. A: Physicochem. 492 (2016) 88–99.
[41] Z. Lu, Q. Liu, Z. Xu, H. Zeng, Probing anisotropic surface properties of molybdenite by direct force measurements, Langmuir 31 (42) (2015) 11409–11418.
[42] B. Kar, H. Sahoo, S.S. Rath, B. Das, Investigations on different starches as depressants for iron ore flotation, Min. Eng. 49 (2013) 1–6.
[43] J.S. Laskowski, Q. Liu, C.T. O'Connor, Current understanding of the mechanism of polysaccharide adsorption at the mineral/aqueous solution interface, Int. J. Miner. Process. 84 (1–4) (2007) 59–68.
[44] A.C. Araujo, P.R.M. Viana, A.E.C. Peres, Reagents in iron ores flotation, Miner. Eng. 18 (2005) 219–224.
[45] F. Nsib, N. Ayed, Y. Chevalier, Dispersion of hematite suspensions with sodium polymethacrylate dispersants in alkaline medium, Colloid Surf. A: Physicochem. 286 (1–3) (2006) 17–26.
[46] M.A. Legodi, D. Waal, The preparation of magnetite, goethite, hematite and maghemite of pigment quality from mill scale iron waste, Dyes Pigm. 74 (2007) 161–168.
[47] B. Klahr, S. Gimenez, F. Fabregat-Santiago, T. Hamann, J. Bisquert, Water oxidation at hematite photoelectrodes: the role of surface states, J. Am. Chem. Soc. 134 (2012) 4294–4302.
[48] C. Du, M. Zhang, J.W. Jang, Y. Liu, G.Y. Liu, D. Wang, Observation and alteration of surface states of hematite photo-electrodes, J. Phys. Chem. C 118 (2014) 17054–17059.